

# Chaotic mixing and transport in a meandering jet flow

S.V. Prants, M.V. Budyansky, M.Yu. Uleysky,

*V.I. Il'ichev Pacific Oceanological Institute*

*of the Russian Academy of Sciences,*

*43 Baltiiskaya ulitsa, 690041 Vladivostok, Russia*

and G.M. Zaslavsky

*Courant Institute of Mathematical Sciences, New York University, 251 Mercer St., New York, NY 10012, USA*

*and Department of Physics, New York University,*

*2-4 Washington Place, New York, NY 10012, USA*

Mixing and transport of passive particles are studied in a simple kinematic model of a meandering jet flow motivated by the problem of lateral mixing and transport in the Gulf Stream. We briefly discuss a model streamfunction, Hamiltonian advection equations, stationary points, and bifurcations. The phase portrait of the chosen model flow in the moving reference frame consists of a central eastward jet, chains of northern and southern circulations, and peripheral westward currents. Under a periodic perturbation of the meander's amplitude, the topology of the phase space is complicated by the presence of chaotic layers and chains of oscillatory and ballistic islands with sticky boundaries immersed into a stochastic sea. Typical chaotic trajectories of advected particles are shown to demonstrate a complicated behavior with long flights in both the directions of motion intermittent with trapping in the circulation cells being stuck to the boundaries of vortex cores and resonant islands. Transport is asymmetric in the sense that mixing between the circulations and the peripheral currents is, in general, different from mixing between the circulations and the jet. The transport properties are characterized by probability distribution functions (PDFs) of durations and lengths of flights. Both the PDFs exhibit at their tails power-law decay with different values of exponents.

PACS numbers: 05.45.Ac; 47.52.+j; 92.10.Ty

## I. INTRODUCTION

Passive particle advection can be considered as a Hamiltonian dynamical problem. Advection in a two-dimensional meandering shear flow, a simple kinematic model of lateral mixing and transport in the Gulf Stream, is an example of a system with  $3/2$  degrees of freedom. The phase space of an advected particle in such a flow is mixed, i.e. it consists of chaotic layers, islands of periodic motion, and layers of periodic open trajectories. All these parts of the phase space influence the transport of passive particles, which can become anomalous if trajectories stick to the boundaries of topological structures with regular dynamics. Particularly the stickiness to the so-called ballistic islands can create flights along the stream flow, make the transport superdiffusive, and influence in a strong way the advected particles distribution.

---

The goal of this paper is to study Lagrangian lateral mixing and transport of passive particles advected by a shear flow that has a coherent space organization with two chains of vortices and a strong jet between them. Temporal perturbations of shear flows are known to induce chaotic mixing. Similar flows occur naturally in the ocean as western boundary currents, like the Gulf Stream in the Atlantic Ocean and the Kuroshio in the Pacific Ocean, separating water masses with different physical and biogeochemical characteristics.

Hamiltonian chaos theory has been widely used to study advection of passive particles in hydrodynamic flows of ideal fluid (for review see [1, 2]). The equations of motion of a passive particle advected by a two dimensional incompressible flow is known to have a Hamiltonian form

$$\begin{aligned}\frac{dx}{dt} &= u(x, y, t) = -\frac{\partial \Psi}{\partial y}, \\ \frac{dy}{dt} &= v(x, y, t) = \frac{\partial \Psi}{\partial x},\end{aligned}\tag{1}$$

with the stream function  $\Psi$  playing the role of a Hamiltonian and the coordinates  $(x, y)$  of a particle playing the role of canonically conjugated variables. Equations (1) form a Hamiltonian dynamical system whose phase space is identified as the physical space of advected particles.

All time-independent one-degree-of-freedom Hamiltonian systems are known to be integrable. It means that all fluid particles move along streamlines of a time-independent streamfunction in a regular way. Equations (1) with a time-periodic streamfunction are usually non-integrable, giving rise to chaotic particle's trajectories. In other words, even regular Eulerian velocity fields  $(u, v)$  can generate chaotic trajectories, the phenomenon known under the names "chaotic advection" or "Lagrangian chaos" [1, 3]. In this field mixing means stretching and deformation of material lines by advection. The term "transport" refers to the motion of passive particles from one region of the physical space to another.

Well developed theory of Hamiltonian chaotic mixing and transport in the phase space (for a review see [4, 5, 6, 7]) has been successfully applied to study chaotic mixing and transport of passive particles in fluids [8, 9, 10, 11, 12, 13, 14, 15, 16, 17, 18, 19, 20]. The phase space of a typical chaotic Hamiltonian system consists of regions of chaotic mixing and regions with regular trajectories. A boundary between them often contains a complicated hierarchical structure of islands with regular trajectories and can be extremely sticky for some values of control parameters [21, 22, 23, 24, 25, 26]. All these properties are manifested in mixing and transport of passive particles in fluids and have been observed in laboratory [27, 28, 29]. Particles in the core regions of regular motion and in the islands are trapped there forever unless we do not take into account molecular diffusion and noise. They do not participate in the transport. So the outermost KAM tori play the role of transport barriers in the fluid. The particles, entering the boundary layer, can spend a very large time there giving rise anomalous transport or anomalous diffusion.

The motion in chaotic regions is extremely sensitive to small variations in initial particle's positions. So one forces to use an statistical approach to describe transport. A commonly used statistical measure of transport is the variance  $\sigma^2(t) = \langle x^2 \rangle$ , which for simplicity is written for the particle displacement in one dimension. The averaging is supposed to be done over an ensemble of particles. If mixing in the phase space would be ideal (as it occurs in a hyperbolic dynamical system with unstable orbits only, whose phase space does not contain any regular islands) the variance would satisfy the law of normal diffusion,  $\sigma^2(t) = 2Dt$ , with a well-defined diffusion coefficient  $D = \lim_{t \rightarrow \infty} \sigma^2/2t$ . If trajectories are dominated by sticking to the boundaries of regular regions, where particles may spend a long time, subdiffusion takes place with the transport law  $\sigma^2(t) \sim t^\mu$ ,  $\mu < 1$ . Superdiffusion with  $\mu > 1$  occurs when particles

execute long “flights”, i.e. travel long distances between (or even without) sticking events. Anomalous diffusion implies the diffusion coefficient  $D$  to be either zero ( $\mu < 1$ ) or infinite ( $\mu > 1$ ). As to transport of advected particles in fluids with diffusion [30] and transport in the phase space in the presence of noise [31, 32], the situation is more complicated. For example, as it is shown in Ref. [30] subdiffusion is not possible in incompressible flows in the presence of molecular diffusivity.

It is as well possible to describe transport in terms of spatial extensions and durations of sticking and/or flight events. The respective probability density functions (PDFs) of durations of flights,  $P(t) \sim t^{-\gamma}$ , and of lengths of flights,  $P(x) \sim x^{-\nu}$ , are expected to be power-law functions. Long-time flights provide a link between chaotic advection and anomalous diffusion. Quantitative connections between all the exponents  $\mu$ ,  $\gamma$ , and  $\nu$  have been established with some simple models of chaotic motion and continuous-time random walks (for a review of anomalous transport see [6, 33, 34, 35]).

To specify the model we choose the shear flow in the form of the Bickley jet [36] with the velocity profile  $\text{sech}^2 y$  and an imposed running wave with the periodically varied amplitude. This model is related to the so-called non-twist Hamiltonians (see [14, 37, 38] and references therein) that have a specific phase space topology and bifurcations with respect to the parameters change. As it usually occurs in Hamiltonian systems, separatrices are destroyed in the presence of an arbitrary small time-dependent perturbation. Instead of them narrow stochastic layers appear which are “seeds” of Hamiltonian chaos. There are an infinite number of nonlinear resonances between the frequency of the perturbation and frequencies of rotations of advected particles. With increasing the strength of the perturbation, more and more of them begin to destroy and overlap. Motion of particles in the regions of the overlapping resonances in the phase space is no more confined by impenetrable barriers of KAM tori and a large-scale transport becomes possible.

In Sec. II we derive equations of motion for passive particles in the moving frame of reference, find stationary points of the flow, topologically different regimes of motion, and bifurcations between them. Similar kinematic models with imposed time-periodic velocity fields have been used in literature on physical oceanography to study lateral Lagrangian mixing and transport in the meandering Gulf Stream current [39, 40, 41]. Mixing has been shown with the help of Poincaré sections to be chaotic in a wide range of the control parameters, and the magnitudes of fluxes have been estimated with the help of the Melnikov integral.

In Sec. III we describe topology of the phase space with regions of regular and chaotic motion of advected particles. Sticking to the boundaries of different types of islands, including ballistic ones, and of the vortex cores is demonstrated on Poincaré sections of the particle’s trajectories. Sec. IV is devoted to quantifying chaotic transport. We compute the statistics of durations and lengths of flights for a number of long-time trajectories and find the transport both in western and eastern directions to be anomalous with different values of the exponents.

## II. MODEL STREAMFUNCTION, STATIONARY POINTS, AND BIFURCATIONS

We take the Bickley jet with a running wave imposed as a model of a meandering shear flow in the ocean [39]. The respective streamfunction in the laboratory frame of reference has the following form:

$$\Psi'(x', y', t') = -\Psi'_0 \tanh \left( \frac{y' - a \cos k(x' - ct')}{\lambda \sqrt{1 + k^2 a^2 \sin^2 k(x' - ct')}} \right), \quad (2)$$

where the hyperbolic tangent produces the velocity profile  $\sim \text{sech}^2 y'$ , the square root provides a possibility to have a homogeneous Bickley jet with the width  $\lambda$ , and  $a$ ,  $k$ , and  $c$  are amplitude, wavenumber, and phase velocity of the wave, respectively. The normalized streamfunction in the frame moving with the phase velocity  $c$  is

$$\Psi = -\tanh \left( \frac{y - A \cos x}{L \sqrt{1 + A^2 \sin^2 x}} \right) + Cy, \quad (3)$$

where  $x = k(x' - ct')$ ,  $y = ky'$ ,  $A = ak$ ,  $L = \lambda k$ , and  $C = c/\Psi'_0 k$ .

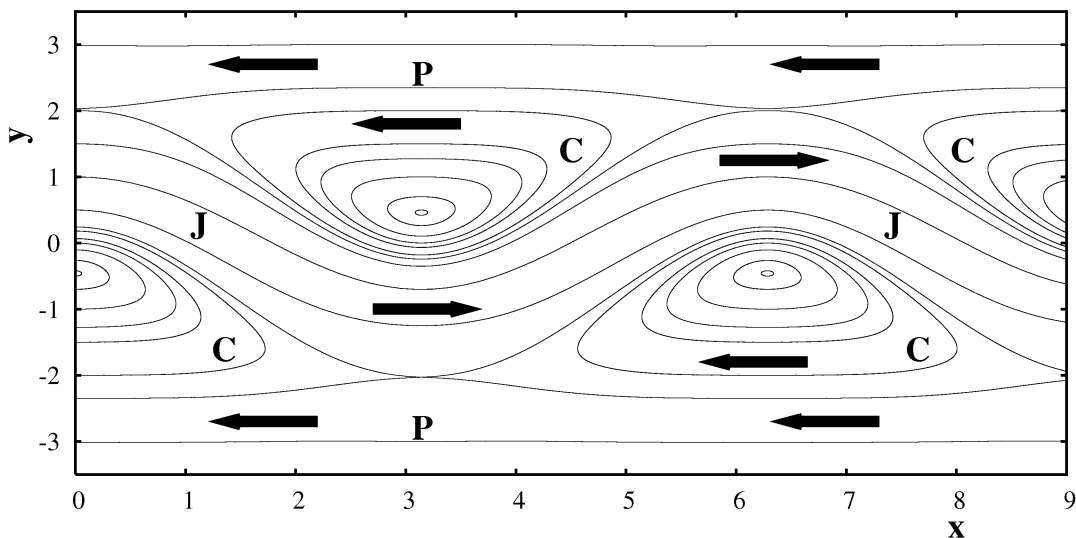


FIG. 1: The phase portrait of the model shear flow (3) in the frame moving with the meander's phase velocity. Streamlines in the circulation (C), jet (J), and peripheral currents (P) zones are shown. The parameters are  $A = 0.785$ ,  $C = 0.1168$ , and  $L = 0.628$ .

The respective advection equations (1) in this moving frame have the form

$$\begin{aligned} \dot{x} &= \frac{1}{L \sqrt{1 + A^2 \sin^2 x} \cosh^2 \theta} - C, \\ \dot{y} &= -\frac{A \sin x (1 + A^2 - Ay \cos x)}{L (1 + A^2 \sin^2 x)^{3/2} \cosh^2 \theta}, \\ \theta &= \frac{y - A \cos x}{L \sqrt{1 + A^2 \sin^2 x}}, \end{aligned} \quad (4)$$

where dot denotes differentiation with respect to dimensionless time  $t = \Psi'_0 k^2 t'$ . The one-degree-of-freedom dynamical system (4) is generated by the Hamiltonian (3) and has three control parameters — the jet's width  $L$ , meander's

amplitude  $A$ , and phase velocity  $C$ . The scaling chosen results in the translational invariance of equations (4) along the  $x$ -axis with the period  $2\pi$ .

A brief description of stability of stationary points and bifurcations of equations (4) is given below. It is clear from the first equation in (4) that stationary points may exist only if the condition  $LC \leq 1$  is fulfilled. Two equalities, following from the second equation in (4)

$$\sin x = 0, \quad 1 + A^2 - Ay \cos x = 0, \quad (5)$$

give four stationary points

$$\begin{aligned} x_{1,2} = 0, \quad y_{1,2} &= \pm L \operatorname{Arcosh} \sqrt{\frac{1}{LC}} + A, \\ x_{3,4} = \pi, \quad y_{3,4} &= \pm L \operatorname{Arcosh} \sqrt{\frac{1}{LC}} - A. \end{aligned} \quad (6)$$

As follows from the stability analysis, the second and third points are always stable whereas the first and fourth ones are stable only if

$$AL \operatorname{Arcosh} \sqrt{\frac{1}{LC}} > 1. \quad (7)$$

It is proved in Ref. [42] that if the condition

$$C < \frac{1}{L \cosh^2(1/AL)} \quad (8)$$

is fulfilled, then there are four new stationary points in equations (4) in addition to the points (6).

Having found the stationary points, their stability properties, and how they are connected, we get the following topologically different phase portraits of the streamfunction (3)

1.  $C > C_{\text{cr1}} = 1/L$ , there are no stationary points.
- 2a.  $C_{\text{cr1}} > C > C_{\text{cr2}} = 1/L \cosh^2(1/AL)$  and  $C > C_{\text{cr3}}$ , there are four stationary points (6): two centers (the second and third ones) and two saddles (the first and fourth ones). There are two separatrices each of which passes through its own saddle. A free flow between the separatrices is westward.
- 2b.  $C_{\text{cr1}} > C > C_{\text{cr2}}$  and  $C < C_{\text{cr3}}$ , the stationary points are the same as in the preceding case, but a free flow between the respective separatrices is eastward.
- 3a.  $C_{\text{cr2}} > C > C_{\text{cr3}}$ , there are eight stationary points: four centers (6) and four saddles with positions found in Ref. [42]. There are two separatrices, each of which connects two saddle points. A free flow between the separatrices is westward.
- 3b.  $C_{\text{cr2}} > C$  and  $C < C_{\text{cr3}}$ , the stationary points are the same as in the preceding case, but a free flow between the respective separatrices is eastward.

Therefore, from the point of view of existence and stability of stationary states, there are three possibilities: 1) there are no stationary points; 2) there are four stationary points, two centers and two saddles; 3) there are eight stationary points, four centers and four saddles. A bifurcation between the first and second regimes consists in arising

two pairs “saddle-center”. A bifurcation between the second and third regimes consists in arising two saddles and a center between them instead of one saddle (a fork-type bifurcation).

There is one more bifurcation that does not change the number and stability of stationary points but changes the topology of the flow. The values of the streamfunction (3) on the separatrices are equal on modulo but of opposite signs. There is a critical value of the phase velocity  $C = C_{cr3}$  under which the separatrices coincide and the respective streamfunction is equal to zero. If  $C > C = C_{cr3}$ , a free flow between the separatrices is westward, whereas with  $C < C = C_{cr3}$  it is eastward. It is difficult to find  $C = C_{cr3}$  analytically but it may be shown [42] that  $C_{cr3} > C_{cr2}$ , if

$$\frac{2(1 + A^2)}{AL \sinh(2/AL)} < 1. \quad (9)$$

Otherwise  $C_{cr3} < C_{cr2}$ .

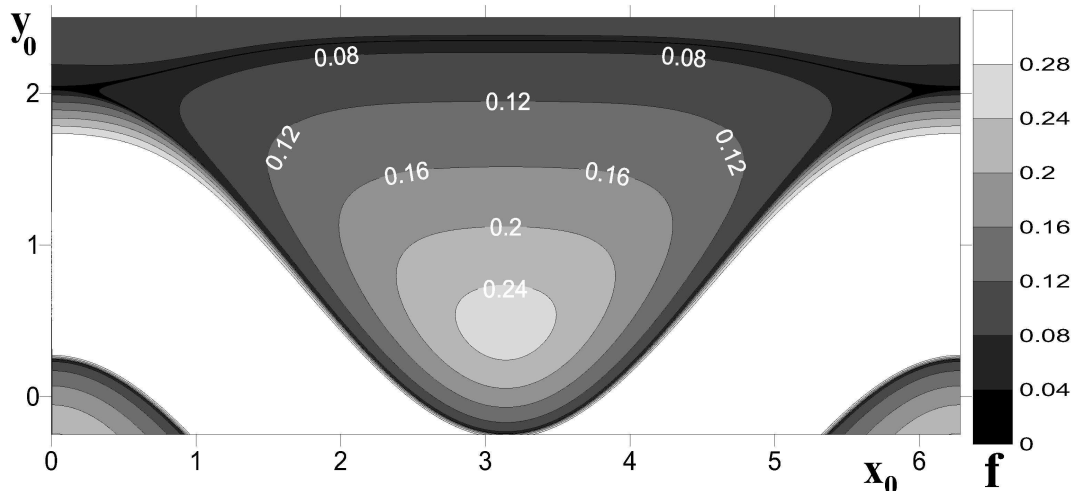


FIG. 2: The frequency map represents by color the values of frequency of rotation  $f$  of particles with initial positions  $(x_0, y_0)$  advected by the unperturbed flow (3).

### III. TOPOLOGY OF THE PHASE SPACE

Being motivated by the boundary oceanic eastward meandering jet currents like the Gulf Stream and the Kuroshio, we will deal further in this paper with the case 2b in the list in the preceding section. The respective phase portrait in the reference frame, moving with the phase velocity of the meander (Fig. 1), consists of three different regions: the central eastward jet ( $J$ ), chains of the northern and southern circulations ( $C$ ), and the peripheral westward currents ( $P$ ). The elliptic points (centers) of the circulations are at critical lines  $y = y_c$  with  $u(y_c) = c$  and  $v(y_c) = 0$ . The northern separatrix connects the saddle points at  $x_1 = 2\pi k$  and  $y_1$  to be defined from equation (6) and the southern one connects the saddle points at  $x_4 = (2k + 1)\pi$  and  $y_4$  from (6), where  $k = 0, \pm 1, \dots$

In the presence of a time dependent perturbation, the separatrices are destroyed and transformed into stochastic layers. As a perturbation, we take the periodic modulation of the meander’s amplitude,  $A = A_0 + \varepsilon \cos(\omega t + \varphi)$ , in the streamfunction (3) written in the frame moving with the phase velocity of the meander. The jet’s width  $L = 0.628$ , the phase velocity  $C = 0.1168$ , and the meander’s amplitude  $A_0 = 0.785$  will be fixed in simulation throughout the

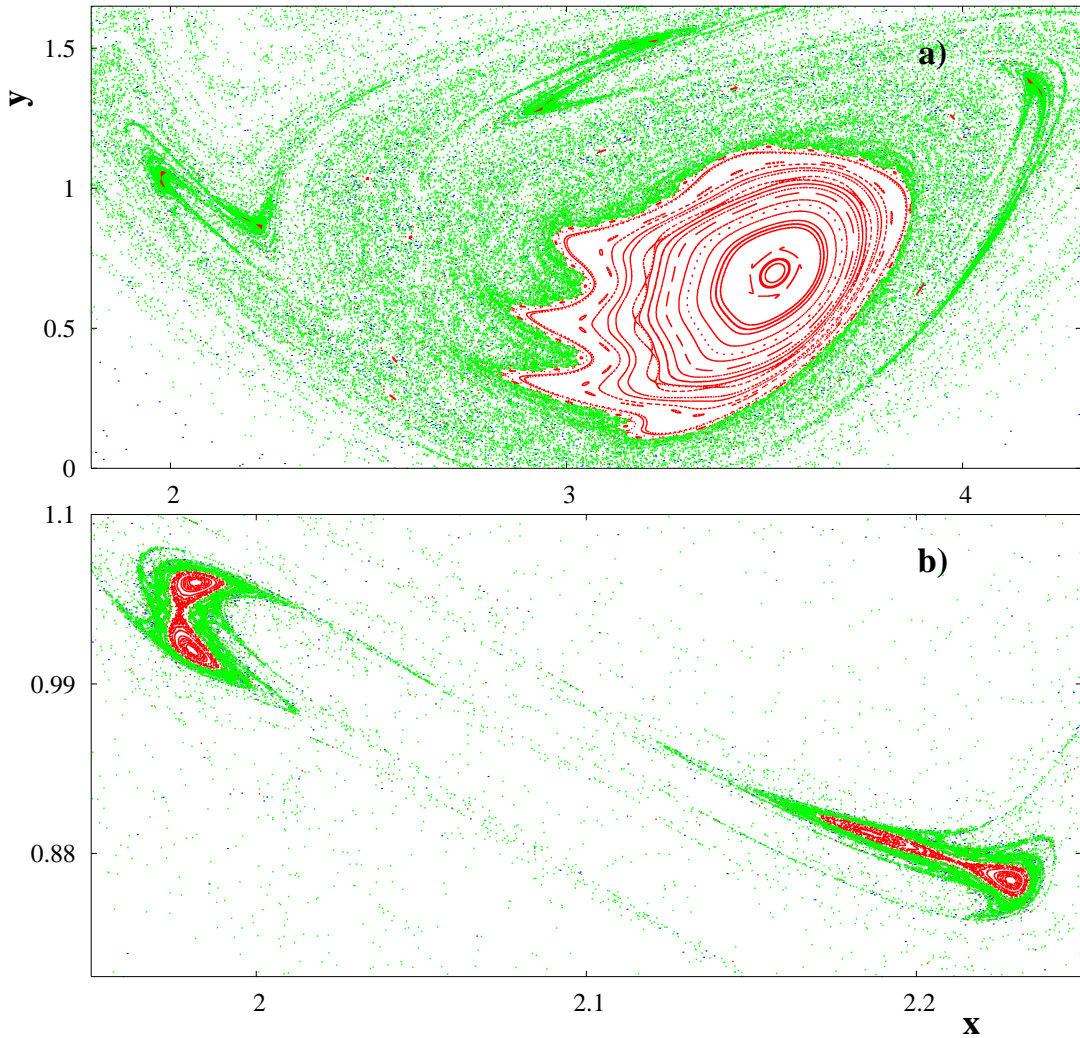


FIG. 3: (color online). Poincaré section of the streamfunction (3) with the same parameters as in Fig. 1 and the amplitude  $\varepsilon = 0.0785$  and frequency of perturbation  $w = 0.2536$ . (a) General view, (b) zoom of a pair of islands of the secondary resonance.

paper. These values are in the range of the parameters which has been estimated [39, 40] to be realistic with the Gulf Stream current.

Changing the strength  $\varepsilon$  and frequency  $\omega$  of the perturbation, we can change the number of overlapping resonances between the perturbation frequency and the frequencies  $f$  of particle's rotations in the circulation zones. In Fig. 2 we plot a frequency map  $f(x_0, y_0)$  that shows by color the values of  $f$  for particles with initial positions  $(x_0, y_0)$  in the unperturbed system.

Let us take the values of the perturbation frequency  $\omega = 0.2536$  to be close to the values of the unperturbed frequency  $f$  in the inner core of the circulation zone and the strength of perturbation to be rather small  $\varepsilon = 0.0785$ . Due to the zonal and meridian symmetries it is possible to consider particle's motion on the cylinder with  $0 \leq x \leq 2\pi$ . The respective Poincaré section for a large number of trajectories is shown in Fig. 3. The vortex core, that survives under this small perturbation, is immersed into a stochastic sea where one can see six islands of a secondary resonance to be emerged from three islands of the primary resonance  $3f = 2\omega$ , where  $f = 0.169$ . A pair of the secondary resonance

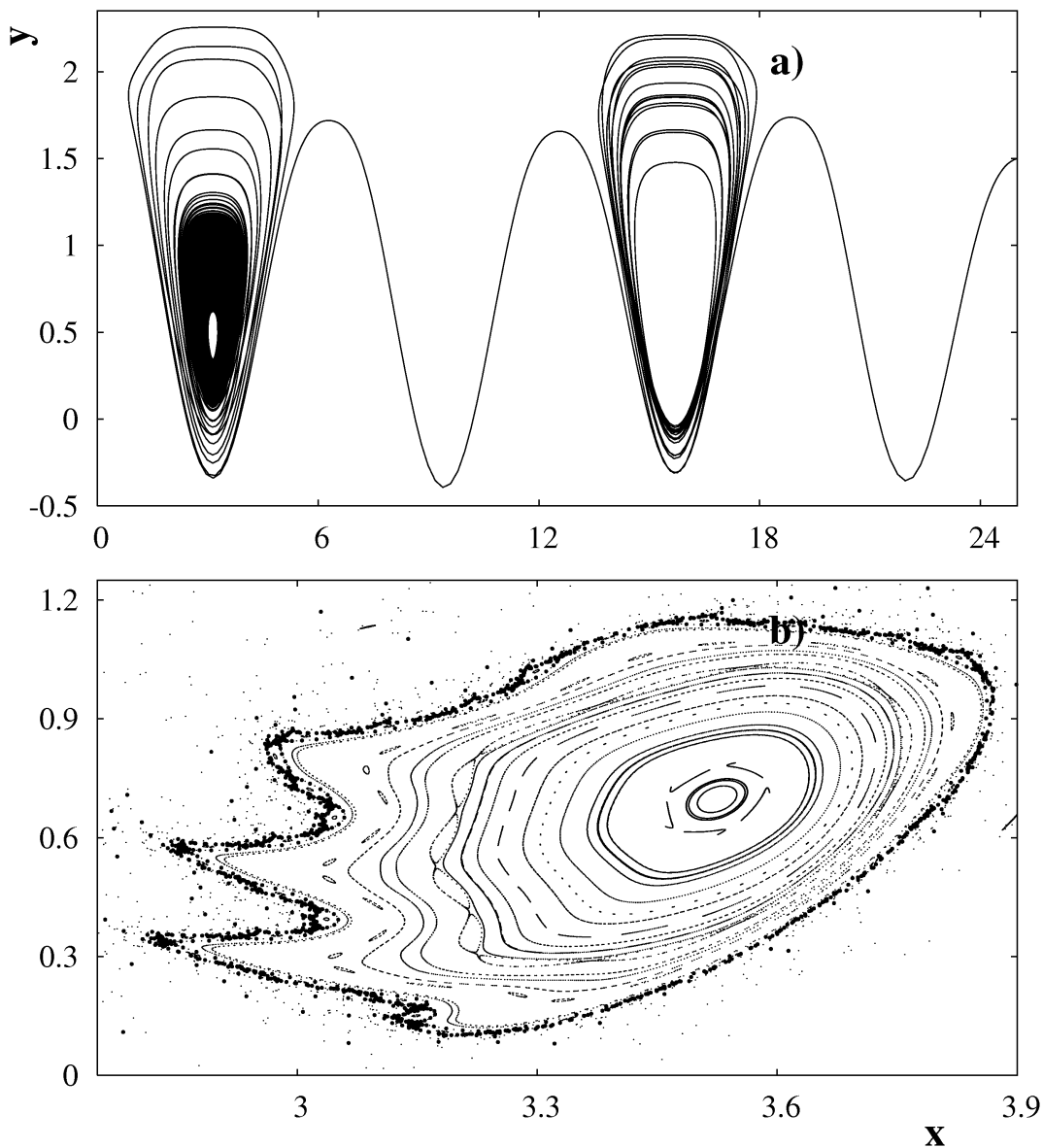


FIG. 4: A single ballistic trajectory (a) sticking to the vortex core (b). Bold dots show particle's positions through the period of the perturbation.

islands is zoomed in Fig. 3b.

Sticking of particles to boundaries between regular and chaotic regions in the phase space is a typical phenomena with chaotic Hamiltonian systems [6, 7, 21, 22, 23, 24]. What is special in chaotic advection, that real fluid parcels may be trapped for a long time near a vortex core and borders of resonant islands. As to the vortex core, we illustrate this phenomenon in Fig. 4, where tracks of a single ballistic trajectory (Fig. 4a) through the period of the perturbation  $2\pi/\omega$  are shown by bold dots (Fig. 4b). In Fig. 5 we plot tracks of another ballistic trajectory (Fig. 5a) sticking to the islands of the secondary resonance.

Besides the resonant islands with particles moving around the elliptic point in the same frame (Fig. 3), we have found so-called ballistic islands situated in the chaotic sea, in the peripheral currents and on the border between the



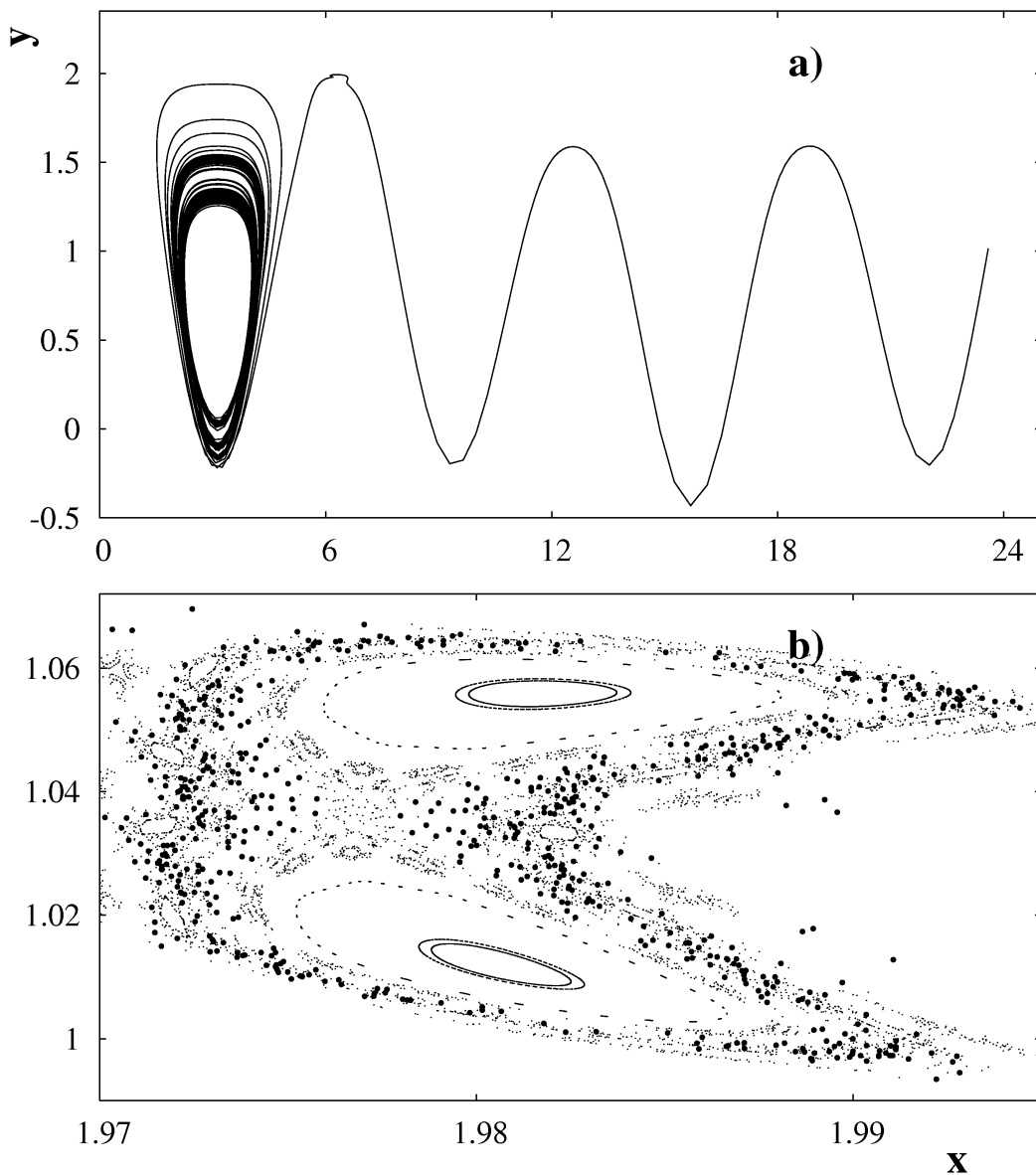


FIG. 5: A single ballistic trajectory (a) sticking to two of the resonant islands of the secondary resonance (b) Bold dots show particle's positions through the period of the perturbation.

chaotic sea and the meandering jet. Ballistic modes [7, 43, 44] correspond to the stable periodic motion of particles from one frame to another. When mapping their positions at the moments of time  $t_k = 2k\pi/\omega$  ( $k=1,2,\dots$ ) onto the first frame, one can see chains of ballistic islands along the stochastic layer that replaces the destroyed separatrix (Fig. 6a). Zoom of one of the ballistic islands and stickiness of a chaotic trajectory to its border are shown in Fig. 6b. In Fig. 7 we demonstrate two different ballistic trajectories. If a particle is placed initially inside the ballistic island, it travels (to the west in this case) in a regular way (see the upper trajectory in Fig. 7a) with practically a constant or slightly modulated zonal velocity (see the lower line in Fig. 7b). The lower trajectory in Fig. 7a on the  $(x, y)$  plane corresponds to a particle placed initially nearby the border of the same ballistic island from the outside. Dependence of its zonal position on time (the upper curve in Fig. 7b) demonstrates clearly an intermittency of flight and sticking

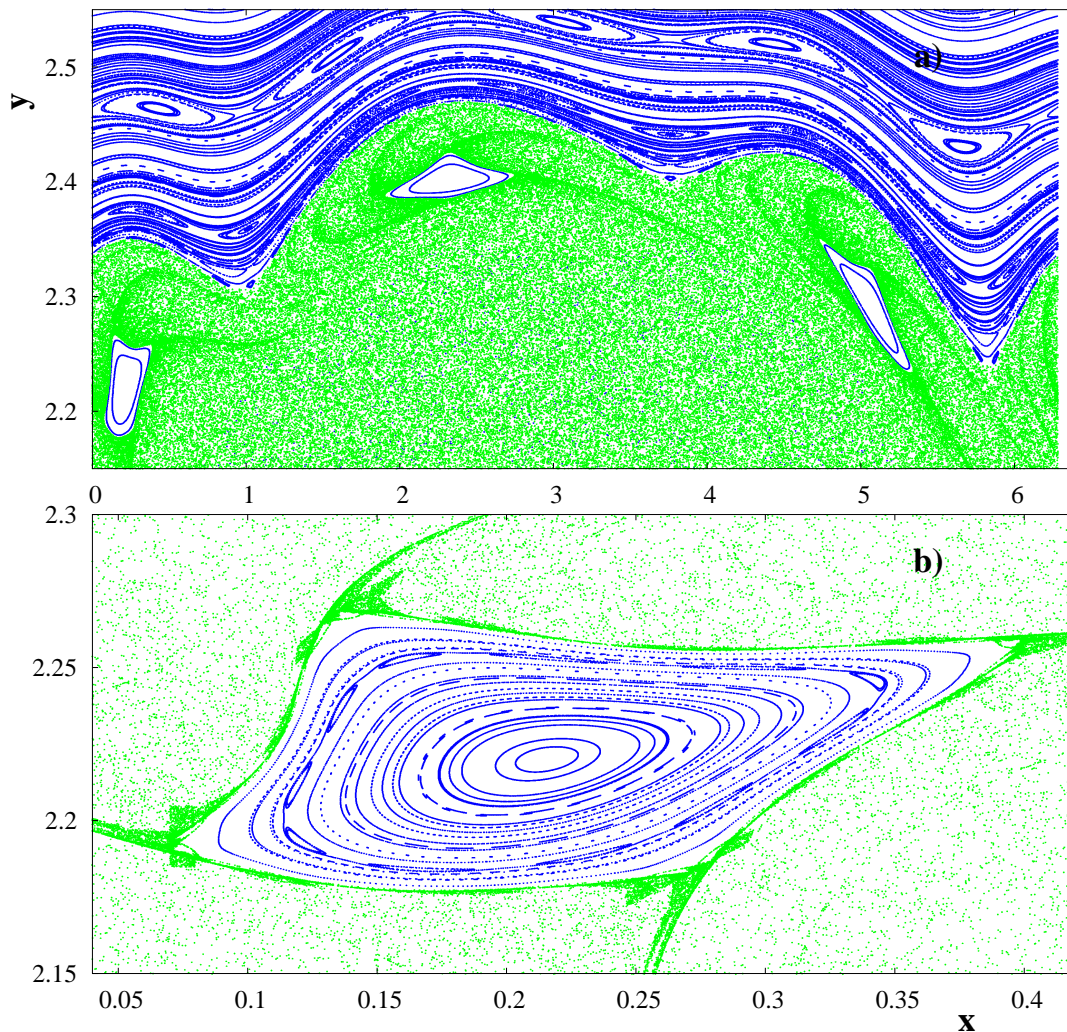


FIG. 6: (color online). (a) Chains of ballistic islands on both sides of the border between the peripheral current and the circulation zone. (b) Zoom of one of the ballistic islands and its sticky border.

events. Stickiness to the islands in Figs. 4 – 6 is shown for different trajectories, for a convenience. Actually, any chaotic trajectory sticks to different islands at different time intervals. Such a behavior one can see in Fig. 7. This type of dynamics complicates its description because of a multifractal nature.

#### IV. CHAOTIC TRANSPORT

With increasing the perturbation strength  $\varepsilon$ , the boundaries (see Fig. 1) between the jet ( $J$ ), circulations ( $C$ ), and peripheral currents ( $P$ ) begin to break down. The vortex core shrinks (see Fig. 3), oscillatory and ballistic islands appear (see Figs. 3 and 6), and a stochastic layer arises instead of the impenetrable transport barrier, the unperturbed separatrix. Passive particles which stick to the boundaries of regular motion can spend there a significant time and deposit to subdiffusion. Those which find themselves in the jet may travel long distances to the east between sticking events, whereas the particles in the peripheral currents travel in the west directions. Because of the absence of the

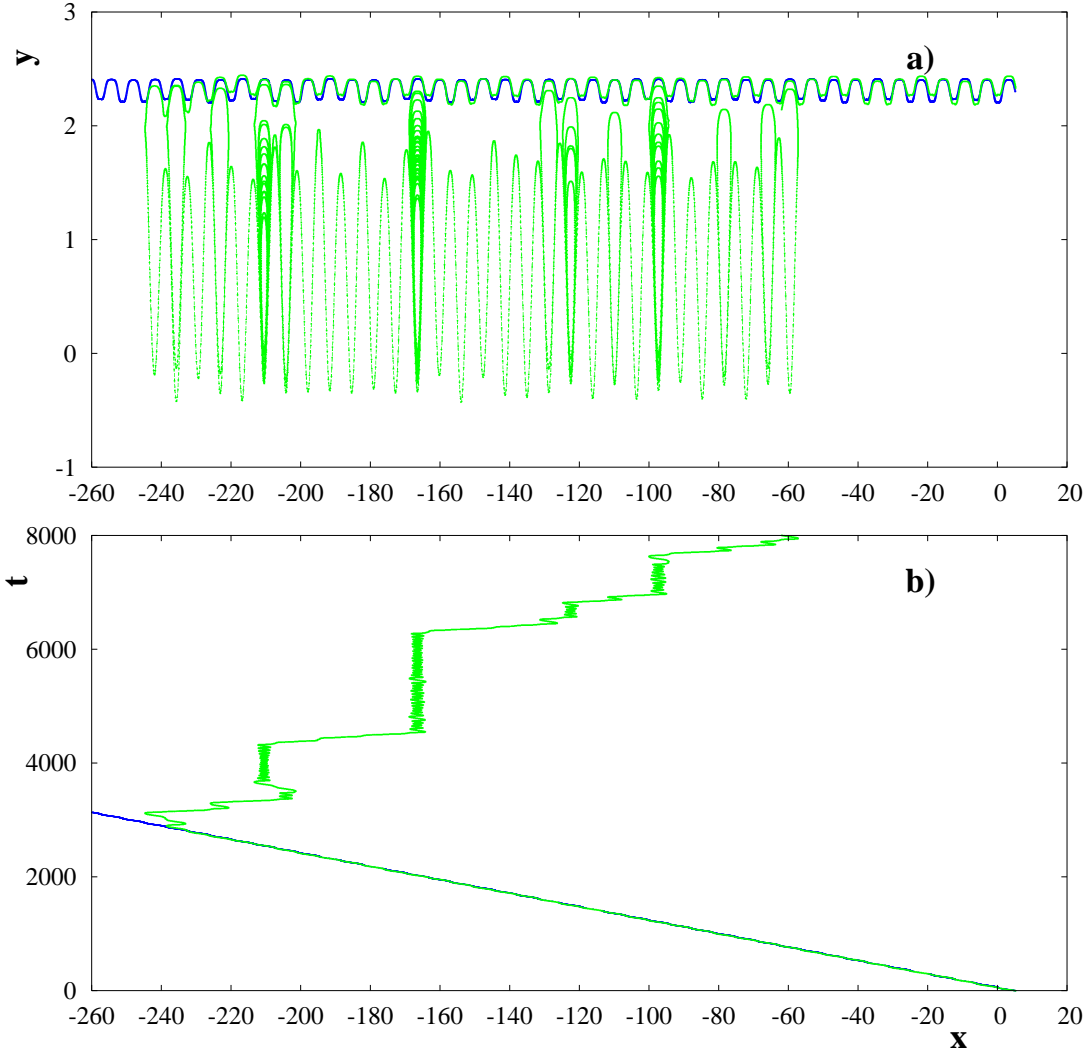


FIG. 7: (color online). Examples of ballistic trajectories (a) on the  $(x, y)$  plane and (b) on the  $(t, x)$  plane. The blue regular trajectory, which is the upper one in (a) and the lower one in (b), is inside a ballistic island. The green chaotic trajectory with close initial position, which is the lower one in (a) and the upper one in (b), demonstrates intermittent sticking and flight events.

former transport barriers, the motion of some particles is intermittent with a large number of turning points at which particles change directions. As usual, we will characterize statistical properties of particles motion by probability distribution functions (PDFs). We will call “a flight” any event between two successive changes of signs of the particle’s zonal velocity. In this terminology a sticking consists of a number of flights with approximately equal flight times. It should be noted that some authors distinguish flights from sticking motion by examining a distance between successive local extrema of trajectories  $x(t)$  [15, 29]. Both the PDF of durations of flights  $P(T_f)$  and of lengths of flights  $P(x_f)$  will be used to characterize the chaotic transport.

The Poincaré section of the flow with the perturbation strength  $\varepsilon = 0.0785$  and frequency  $\omega = 0.2536$  is shown in Fig. 3a. The flight PDFs are computed with 6 particles (initially placed in the first east frame inside a stochastic layer) up to the long time  $t = 5 \cdot 10^8$  and with 125 particles up to  $t = 5 \cdot 10^6$ . Particles inside the stochastic layer

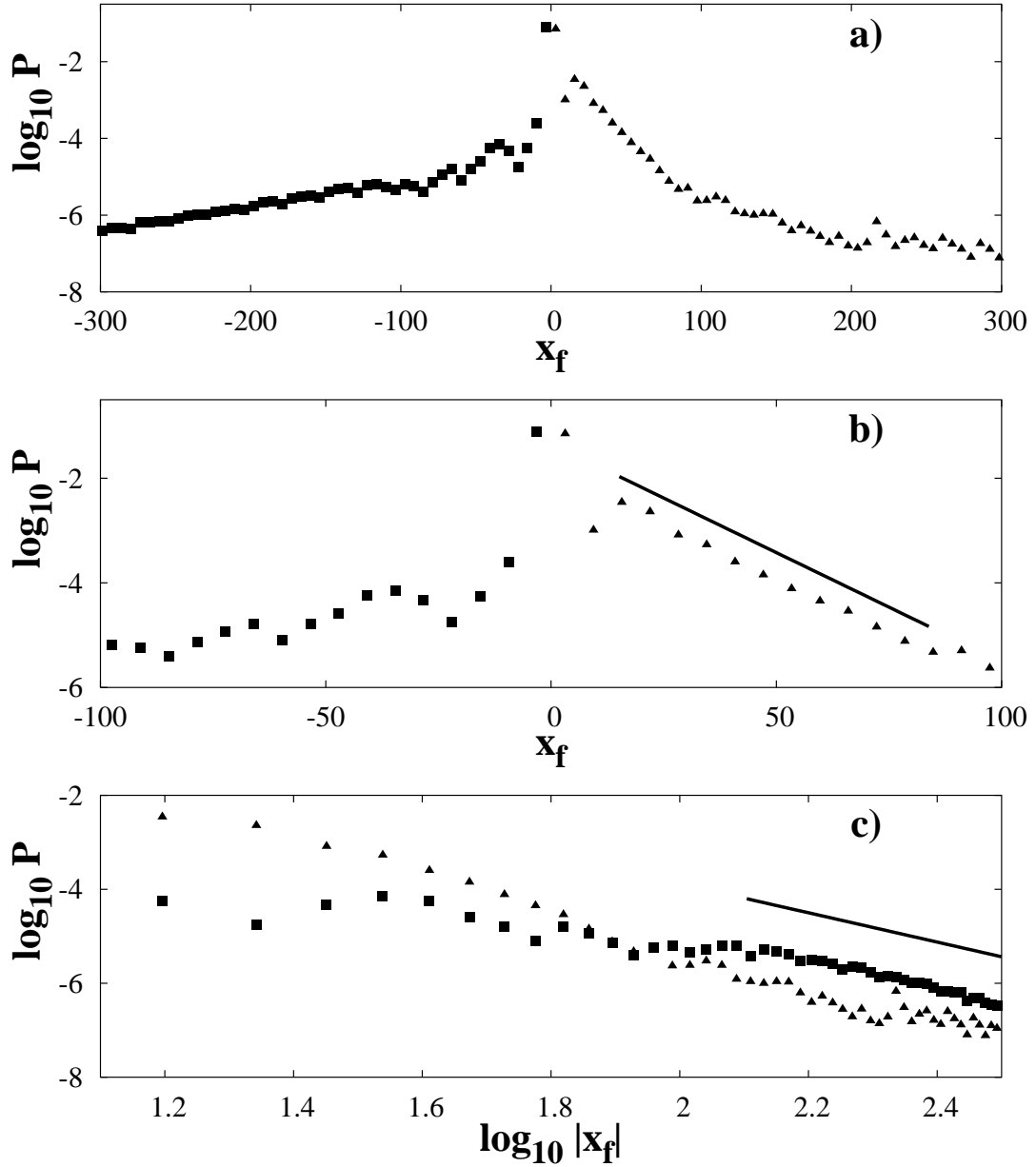


FIG. 8: (a) Probability distribution functions (PDFs) of lengths of eastward (triangles) and westward (squares) flights obtained with 6 chaotic trajectories for  $5 \cdot 10^8$  steps. (b) For short eastward flights,  $15 \leq x_f \leq 85$ , the PDF decays exponentially, whereas the PDF for westward flights oscillates in the same range. (c) The PDF tail of lengths of westward (squares) long flights decays as a power law with the slope  $\nu = 3.12 \pm 0.1$ .

may execute very complicated motion changing the direction in a chaotic way, sticking to the island's boundaries and executing ballistic flights with different values of length and duration.

The PDF of the lengths of flights is shown in Fig. 8a for both the directions. The asymmetry between the eastward (shown by triangles) and westward (shown by squares) flights is evident. The transport velocity in the peripheral currents is different from the transport velocity in the jet. Mixing between the circulations and the peripheral currents is, in general, different from mixing between the circulations and the jet. Both the PDFs can be roughly split into three distinctive regions. The very short flights with small values of  $|x_f|$  ( $< 2\pi$ ) are supposed to be dominated by

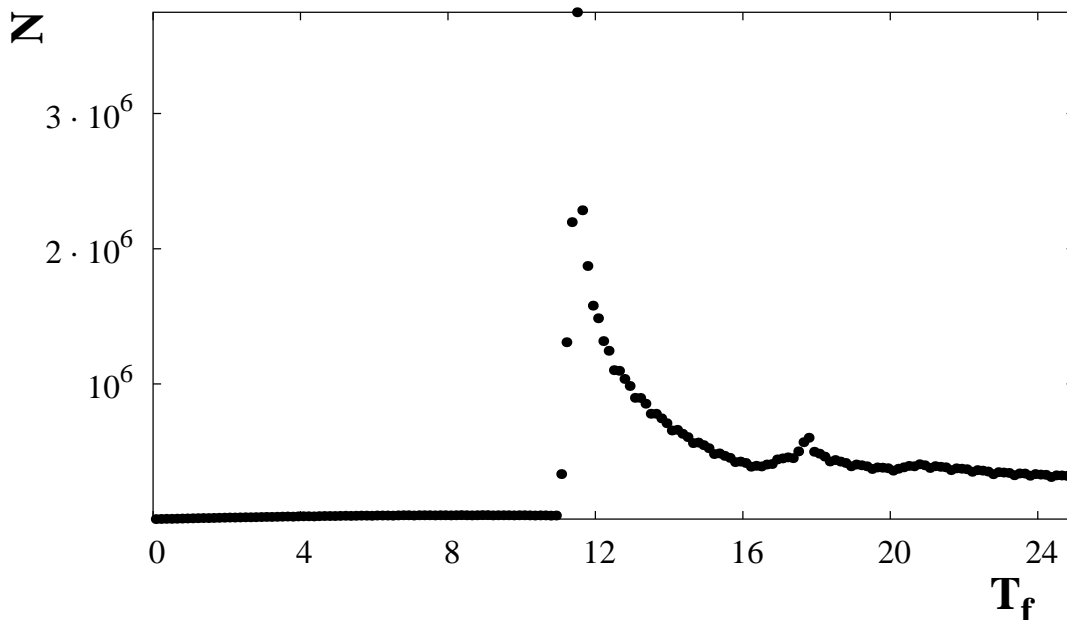


FIG. 9: The number of particles  $N$  executing short flights with  $|x_f| < 2\pi$  and a fixed duration  $T_f$ . Peaks at  $T_f \simeq 11.8$  and  $T_f \simeq 18$  correspond to particles sticking to the boundaries of the vortex core and oscillatory islands.

sticking to the boundaries of the vortex core and oscillatory islands. To check that we plot in Fig. 9 the number of particles  $N$  executing short flights with small values of  $T_f$  and with the lengths of flights  $|x_f| < 2\pi$ . The prominent peaks at  $T_f \simeq 11.8$  and  $T_f \simeq 18$  correspond to those particles which stick to the vortex core and resonant island's boundaries (see Fig. 3 and 4). The PDF for eastward flights with the lengths in the range  $15 \leq x_f \leq 85$  decays exponentially, whereas the PDF for westward flights is an oscillating function in this range (see Fig. 8b). The tails of both the PDFs are close to a power-law decay  $P_f(x) \sim |x|^{-\nu}$ . In Fig. 8c we estimate the exponent for long westward flights with corresponding error by least-square fitting of the straight line to the log-log plot of the data to be  $\nu = 3.12 \pm 0.1$ . The tail for long eastward flights in the same range is an oscillating function whose slope is difficult to measure because of insufficient statistics. Simulation with 125 initial conditions up to the time  $t = 5 \cdot 10^6$  shows practically the same results.

The PDF of durations  $T_f$  of eastward flights is shown in Fig. 10 with different number of trajectories to be computed and up to different times. In Fig. 10a we plot the time PDF with 125 chaotic trajectories for  $5 \cdot 10^6$  steps. The exponent of the function  $P_f(t) \sim t^{-\gamma}$  is estimated to be  $\gamma = 2.43 \pm 0.1$  in the range from  $\log_{10} T_f = 2.75$  to  $\log_{10} T_f = 3.8$ . In Fig. 10b the time PDF is plotted with 6 chaotic trajectories but for much longer times  $5 \cdot 10^8$ . The respective exponent is estimated to be practically the same,  $\gamma = 2.48 \pm 0.05$ . What is remarkable is that both the time PDFs demonstrate at the very tails periodic oscillations in the logarithmic scale. That is a common feature with time distribution functions in typical Hamiltonian systems [6, 7, 15]. One of the possible explanations of this fact is existence of a fractal-like hierarchy of islands [6] and a discrete renormalization group [45]. The respective PDF of durations of westward flights is shown in Fig. 11 with 125 chaotic trajectories for  $5 \cdot 10^6$  steps (Fig. 11a) and with 6 chaotic trajectories for  $5 \cdot 10^8$  steps (Fig. 11b). The single algebraic tail is not so evident with westward flights as with eastern ones. Rather one can see in this case more prominent log-periodic oscillations.

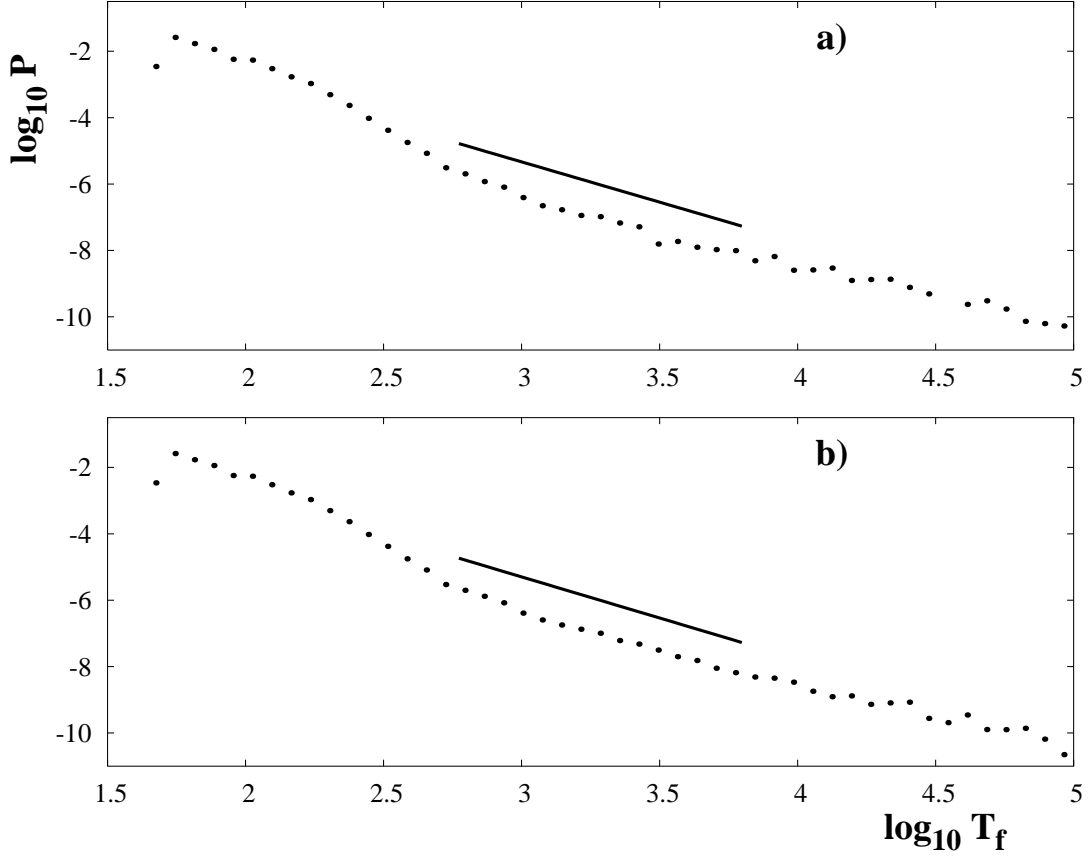


FIG. 10: The PDF of durations of eastward flights (a) with 125 chaotic trajectories for  $5 \cdot 10^6$  steps (the slope is  $\gamma = 2.43 \pm 0.1$ ) and (b) with 6 chaotic trajectories for  $5 \cdot 10^8$  steps (the slope is  $\gamma = 2.48 \pm 0.05$ ).

As it is seen from Fig. 10, the flight-time distribution  $P_f(t)$  has the asymptotic

$$P_f(t) = \frac{\text{const}}{t^\gamma}. \quad (10)$$

One can consider it as an intermediate asymptotic depending on which set of sticky islands it represents. We can expect a fairly complicate multifractal dependence of  $P_f$  on  $t$  and the simplified formula (10) should be applied to specific interval of time and parameters (see more discussion in Refs. [6, 7]). Another approach to study the stickiness is to consider a distribution of Poincaré recurrences of trajectories  $P_{\text{rec}}(t, B)$  to a small domain  $B$  taken in a stochastic sea far enough from sticky domains. It was shown in Refs. [6, 7] that for many different models of chaotic Hamiltonian dynamics the stickiness leads to a distribution of density probability to find the recurrence time within the interval  $(t, t + dt)$ :

$$P_{\text{rec}}(t, B) = \frac{\text{const}}{t^{\gamma^{\text{rec}}}}, \quad (11)$$

where  $\gamma^{\text{rec}} = \min \gamma, (t \rightarrow \infty)$ . From Fig. 10 we have  $\gamma = 2.43 \pm 0.1$  and  $\gamma = 2.48 \pm 0.05$ . This result is consistent with the Kac lemma [6, 7] that imposes  $\gamma > 2$ .

A typical chaotic particle in a stochastic layer changes many times its direction (the sign of the zonal velocity  $u$ ). We have found that the respective turning points are in a narrow strip confined by the curves to be defined by the unperturbed equations of motion (4) with  $\dot{x} = 0$  and  $A = A_0 \pm \varepsilon$ . As an example, we demonstrate in Fig. 12a (color

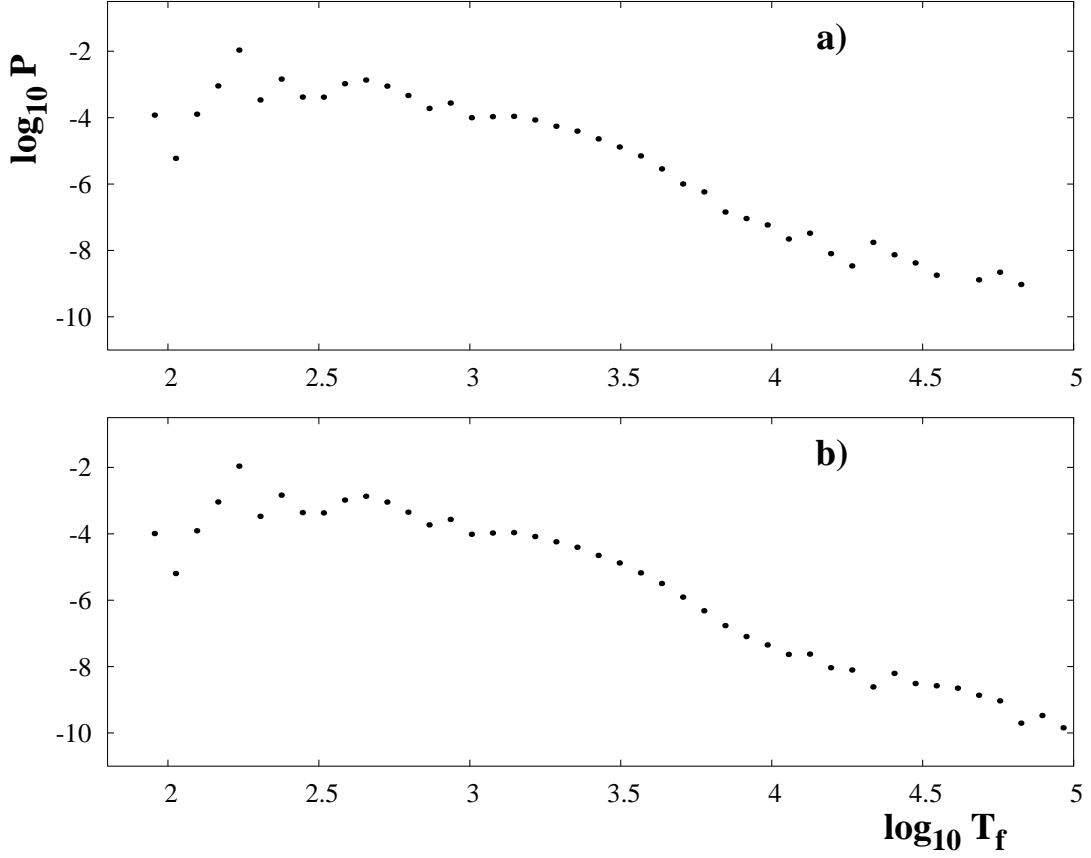


FIG. 11: The PDF of durations of westward flights (a) with 125 chaotic trajectories for  $5 \cdot 10^6$  steps and (b) with 6 chaotic trajectories for  $5 \cdot 10^8$  steps.

online) a narrow strip of red turning points confined by the curves with  $A_0 = 0.785$  and  $\varepsilon = 0.0785$ . All these points belong to a single chaotic trajectory on the cylinder  $0 \leq x \leq 2\pi$ . Figure 12b provides a zoom of the lower part of the strip with the confining curves

$$y = L\sqrt{1 + A^2 \sin^2 x} \operatorname{Arcosh} \sqrt{\frac{1}{LC\sqrt{1 + A^2 \sin^2 x}}} + A \cos x \quad (12)$$

and  $A = A_0 \pm \varepsilon$  to be shown by black solid lines and three regular trajectories to be shown by different colors. The empty part of the strip corresponds to the place where the vortex core is situated (see Fig. 3a).

## V. CONCLUSION

In this paper we have investigated mixing and transport of passive particles in a two-dimensional nonstationary shear flow of the ideal fluid that is relevant to study of mixing of water masses along with their properties in jet-like western boundary currents in the oceans.

We have considered a known kinematic model of a meandering  $\operatorname{sech}^2$  zonal flow [39, 40], derived the respective advection equations in the reference frame, moving with the phase velocity of the meander, found the stationary points and their stability, and possible bifurcations. The control parameters of the model streamfunction (3), the

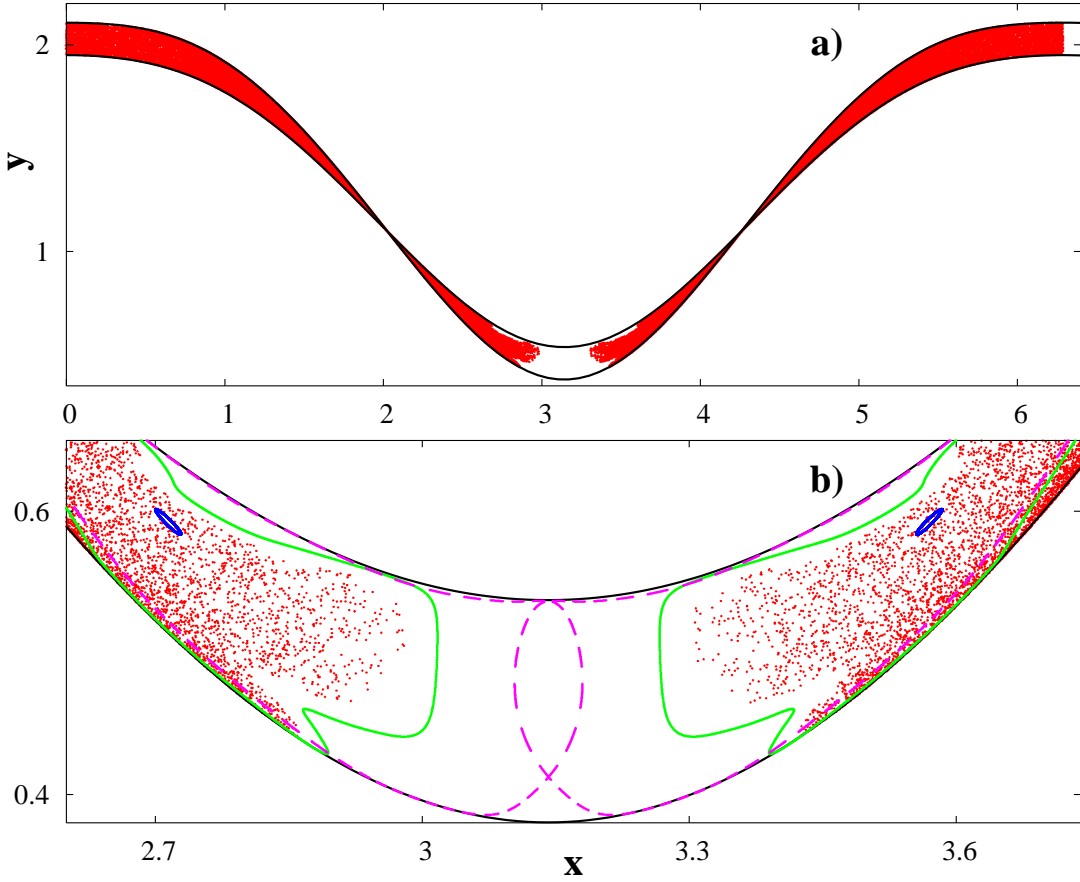


FIG. 12: (color online). Turning points (red ones online) of a single chaotic trajectory on the cylinder  $0 \leq x \leq 2\pi$  are in a narrow strip confined by two curves with equations  $y = f(x)$  to be defined in the text. (a) General view. (b) Zoom with a few regular trajectories shown for reference.

scaled jet's width  $L = 0.628$ , the phase velocity  $C = 0.1168$ , and the meander's amplitude  $A = 0.785$ , were chosen to correspond to estimated realistic values of the Gulf Stream meander's parameters [39, 40] and to the topology of the flow with two chains of circulation cells separated by an eastward jet (the case 2b in the list of possible flow regimes in Sec. II).

The respective phase space has been shown to consist of the vortex cores filled with regular trajectories surrounded by a chaotic sea with stochastic layers and chains of islands of oscillatory and ballistic regular motion. The boundaries of these regular structures have been shown to be sticky. Typical advected particles may alternate chaotically between being trapped near the vortex cores and island's boundaries and "flying" freely in the jet.

Defining "a flight" as an event between two successive changes of signs of the particle's zonal velocity, we characterize the statistics of flights by the PDFs computing both the PDF of durations of the flights  $P_f(t)$  and of lengths of the flights  $P_f(x)$ . Both the functions have been found to have regions with different laws. For short flights we have found two peaks in the  $P_f(x)$  function corresponding to sticking events in the circulations, for middle flights an exponential decay has been found, and the tails with long flights has been found to fit to a power law. An asymmetry of transport of passive particles in the eastern and western directions is caused by a difference in mixing between the circulations and the peripheral currents and mixing between the circulations and the jet. The tails of the time PDFs for eastern



and western flights have been shown to be close to power-law decay functions. The anomalous statistics of the flights is caused by the coherent structures – the circulation cells, the peripheral currents, and the jet – where particles can spend an anomalous amount of time either being trapped in the circulations or moving in the peripheral currents and in the jet.

### Acknowledgments

S.P., M.B., and M.U. were supported by the Russian Foundation for Basic Research (Grant no.06-05-96032), by the Program “Mathematical Methods in Nonlinear Dynamics” of the Russian Academy of Sciences and by the Program for Basic Research of the Far Eastern Division of the Russian Academy of Sciences. G.Z. and S.P. were supported by the ONR Grant no. N00014-02-1-0056 and the NSF Grant no. DMS-0417800.

- 
- [1] H. Aref, *Phys. Fluids* **14**, 1315 (2002).
  - [2] J.M. Ottino, *The Kinematics of Mixing: Stretching, Chaos, and Transport* (Cambridge University Press, Cambridge, 1989).
  - [3] H. Aref, *J. Fluid. Mech.* **143**, 1 (1984).
  - [4] V.I. Arnold, V.V. Kozlov, and A.I. Neishtadt, *Mathematical Aspects of Classical and Celestial Mechanics*, in “Encyclopedia of Mathematical Sciences. Dynamical Systems”, v. 3 (Springer, Berlin, 1988).
  - [5] R.S. MacKay and J.D. Meiss (eds.), *Hamiltonian Dynamical Systems — A Reprint Selection* (Adam Hilger, Bristol, 1987).
  - [6] G.M. Zaslavsky, *Phys. Rep.* **371**, 461 (2002).
  - [7] G.M. Zaslavsky, *Hamiltonian Chaos and Fractional Dynamics* (Oxford University Press, Oxford, 2005).
  - [8] V. Rom-Kedar, F. Leonard, and S.J. Wiggins, *J. Fluid Mech.* **214** 347 (1990).
  - [9] J.B. Weiss and E. Knobloch, *Phys. Rev. A* **40**, 2579 (1989).
  - [10] R.T. Pierrehumbert, *Phys. Fluids A* **3**, 1250 (1991).
  - [11] A. Crisanti, M. Falcioni, G. Paladin, and A. Vulpiani, *Riv. Nuovo Cimento* **14**, 1 (1991).
  - [12] T. Bohr, M.H. Jensen, G. Paladin, and A. Vulpiani, *Dynamical Systems Approach to Turbulence* (Cambridge University Press, Cambridge, 1998).
  - [13] G.M. Zaslavsky, D. Stevens, and H. Weitzner, *Phys Rev. E* **48**, 1683 (1993).
  - [14] D. del-Castillo-Negrete and P.J. Morrison, *Phys. Fluids A* **5**, 948 (1993).
  - [15] S. Kovalyov, *Chaos* **10**, 153 (2000).
  - [16] P. Beyer and S. Benkadda, *Chaos* **11**, 774 (2001).
  - [17] M.V. Budyansky, M.Yu. Uleysky, and S.V. Prants, *DAN Earth Science* **382**, 106 (2002) [*Dokl. Akad. Nauk* **382**, 394 (2002)].
  - [18] M.V. Budyansky, M.Yu. Uleysky, and S.V. Prants, *J. Exper. Theor. Phys.* **99**, 1018 (2004) [*Zh. Eksp. Teor. Fiz.* **126**, 1167 (2004)].
  - [19] X. Leoncini, O. Agullo, S. Benkadda, and G.M. Zaslavsky, *Phys Rev. E* **72**, 026218 (2005).
  - [20] T. Benzekri, C. Chandre, X. Leoncini, R. Lima, and M. Vittot, *Phys. Rev. Lett.* **96**, 124503 (2006).
  - [21] C.F.F. Karney, *Physica D* **8**, 360 (1983).
  - [22] B.V. Chirikov and D.L. Shepelyanski, *Physica D* **13**, 394 (1984).
  - [23] J.D. Meiss, *Rev. Mod. Phys.* **64**, 795 (1992).
  - [24] V.V. Beloshapkin and G.M. Zaslavsky, *Phys. Lett. A* **97**, 121 (1993).

- [25] S. Benkadda, S. Kassibrakis, R. White, and G. Zaslavsky, *Phys. Rev. E.* **55**, 4909 (1997).
- [26] N.-C. Panoiu, *Chaos* **10**, 166 (2000).
- [27] J. Sommeria, S.D. Meyers, and H.L. Swinney, *Nature (London)* **337**, 58 (1989).
- [28] T.H. Solomon, E.R. Weeks, and H.L. Swinney, *Phys. Rev. Lett.* **71**, 3975 (1993).
- [29] T.H. Solomon, E.R. Weeks, and H.L. Swinney, *Physica D* **76**, 70 (1994).
- [30] L. Biferale, A. Crisanti, M. Vergassola, and A. Vulpiani, *Phys. Fluids A* **7**, 2725 (1995).
- [31] C.F.F. Karney, A.B. Rechester, and B.R. White, *Physica D* **4**, 425 (1982).
- [32] I. Mezic and S. Wiggins, *Phys. Rev. E* **52**, 3215 (1995).
- [33] E.W. Montroll and M.F. Shlesinger, in *Studies in Statistical Mechanics*, eds. J. Lebowitz and E. Montroll. (North-Holland, Amsterdam, 1984), Vol.11, p.1.
- [34] M.F. Shlesinger, G. M. Zaslavsky, and J. Klafter, *Nature (London)* **363**, 31 (1993).
- [35] R. Metzler and J. Klafter, *Phys. Rep.* **339**, 1 (2000).
- [36] W.C. Bickley, *Phil. Mag.* **23**, 727 (1937).
- [37] J.E. Howard and J. Humpherys, *Physica D* **80** 256 (1995).
- [38] C. Simó, *Regular and Chaotic Dynamics* **3** 180 (1998).
- [39] A.S. Bower, *J. Phys. Oceanogr.* **21**, 173 (1989).
- [40] R.M. Samelson, *J. Phys. Oceanogr.* **22**, 431 (1992).
- [41] S. Dutkiewicz, and N. Paldor, *J. Phys. Oceanogr.* **24**, 2418 (1994).
- [42] M.Yu. Uleysky, M.V. Budyansky, and S.V. Prants, *Nelineinaya Dinamika*, v. 1 (2006) (in press).
- [43] V. Rom-Kedar and G. Zaslavsky, *Chaos* **9**, 697 (1999).
- [44] A. Iomin, D. Gangardt, and S. Fishman, *Phys. Rev. E.* **57**, 4054 (1998).
- [45] D. Sornette, *Phys. Rep.* **297**, 239 (1998).